JACS
JOURNAL OF THE AMERICAN CHEMICAL SOCIETY

Communication

pubs.acs.org/JACS

Polytypism and Unique Site Preference in LiZnSb: A Superior Thermoelectric Reveals Its True Colors

Miles A. White,[†] Gordon J. Miller,*[,†,‡] and Javier Vela*[,†,‡]

[†]Department of Chemistry, Iowa State University, Ames, Iowa 50011, United States

[‡]U.S. DOE Ames Laboratory, Ames, Iowa 50011, United States

Supporting Information

ABSTRACT: The first example of polytypism in the I−II−V semiconductors has been demonstrated with the synthesis of cubic LiZnSb by a low-temperature solution-phase method. This phase exhibits a unique coloring pattern that is novel for this class of compounds. The choice of site configuration has a considerable impact on the band structure of these materials, which in turn affects the transport properties. While the hexagonal polytype has been suggested as a promising n-type and extremely poor p-type thermoelectric material, the cubic analogue is calculated to have high efficiencies for both the n- and p-type derivatives (1.64 and 1.43, respectively, at 600 K). Furthermore, the cubic phase is found to be the energetically favored polytype. This surprising result provides a rationale for the lack of success in synthesizing the hexagonal polytype in either stoichiometric or n-type compositions.

Thermoelectric materials offer an attractive means of generating electricity from heat that would otherwise be wasted. However, thermoelectrics have failed to reach large-scale commercialization because of their relatively high cost and low device efficiency. The challenge with enhancing thermoelectric performance (given by the figure of merit, zT) arises from having to optimize three concordant properties (Seebeck coefficient S, electrical conductivity σ, and thermal conductivity κ), all of which are dependent on the carrier concentration.[1] While this problem makes it difficult to intuitively increase the zT value, recent computational work shows promise in predicting new thermoelectric materials.[2] Among those suggested, lightly doped n-type (0.01 electron/unit cell) LiZnSb was calculated to have $zT \sim 2$ at 600 K.[3] However, the syntheses of n-type LiZnSb attempted to date resulted in unintentionally doped p-type LiZnSb with $zT < 0.1$.[4] Nevertheless, the experimental transport properties measured for this material were in good agreement with ab initio calculations, increasing the likelihood that the n-type analogue will have a high zT. In order to synthesize n-type LiZnSb, an alternative method is necessary to avoid unintentionally doped compositions at the commonly used annealing temperatures.

A potentially promising approach to synthesize LiZnSb is to use solution-phase techniques. The advantages of this method would be twofold. First, hot injection is likely to result in reduced particle size, which has been shown to lower the thermal conductivity and, with it, to increase the thermoelectric efficiency. Second, precursor manipulation can provide better synthetic control compared with traditional solid-state synthesis.[5]

Building upon the recent solution-phase synthesis of a related I−II−V semiconductor (collectively termed Nowotny−Juza phases),[6] we report the solution-phase synthesis of LiZnSb (Figure 1 and Scheme S1). Briefly, diethylzinc (0.2 mmol) and

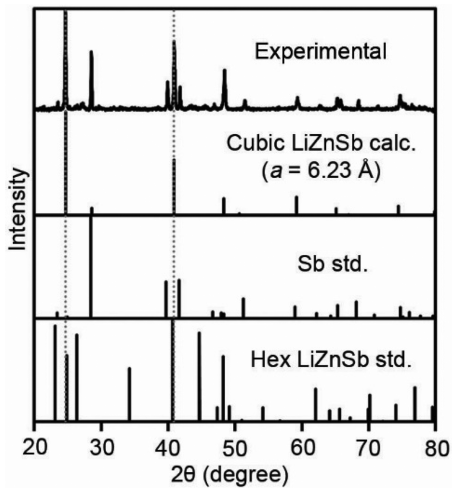

Figure 1. Experimental powder X-ray diffraction pattern of cubic LiZnSb (top panel). Also shown are the calculated pattern of cubic LiZnSb (majority, a = 6.23 Å) and the reference patterns of antimony metal (byproduct) and the previously known hexagonal LiZnSb (unobserved). More information pertaining to the observed and calculated reflections can be found in Table S1.

n-butyllithium (0.2 mmol) were injected in quick succession into a flask containing triphenylstibine (2.0 mmol) in 1-octadecene (5 mL) at 250 °C, after which the mixture was heated to 300 °C for 4 h. Despite prior literature reports that bulk LiZnSb made by solid-state synthesis exhibits a hexagonal structure, LiZnSb synthesized by this solution-phase method exhibits a previously unknown cubic structure (a = 6.23 Å from Rietveld refinement), making it the first example of polytypism within the Nowotny−Juza phases. Furthermore, when lightly doped (<0.02 carriers/unit cell), n-type and p-type forms of this material are calculated to exhibit exceptional zT values of 1.64 and 1.43, respectively, at 600 K.

Received: September 24, 2016
Published: October 21, 2016

DOI: 10.1021/jacs.6b10054
J. Am. Chem. Soc. 2016, 138, 14574−14577

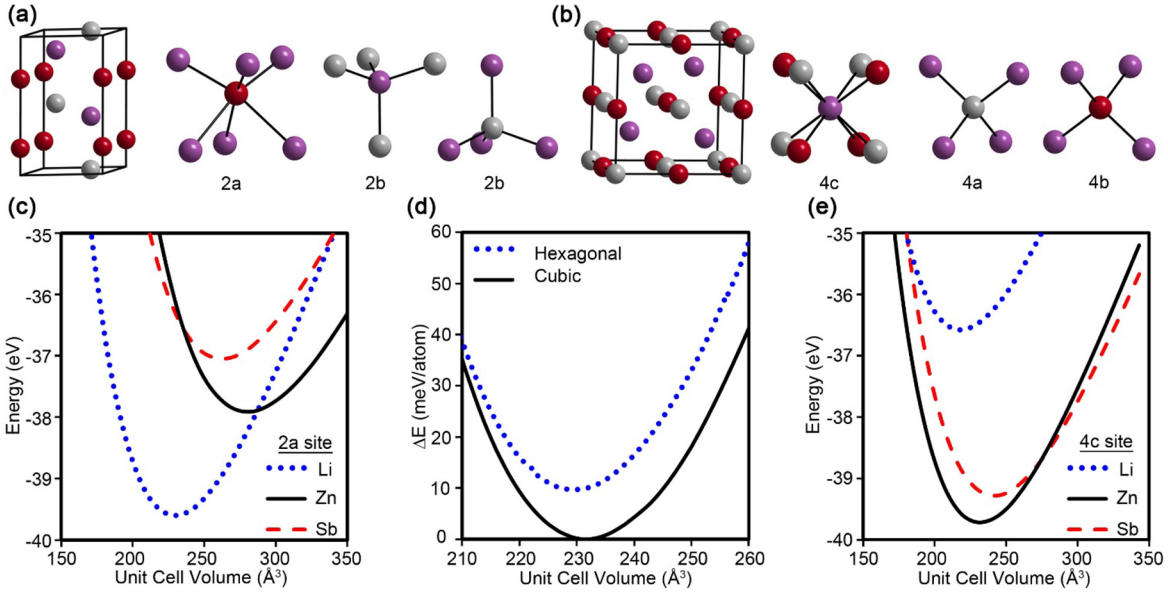

Figure 2. (a, b) Unit cells and local environments for (a) hexagonal and (b) cubic LiZnSb polytypes. The unique crystallographic sites that impact the total energy with coloring are the 2a and 4c sites in the hexagonal and cubic unit cells, respectively. (c, e) Energy vs volume ($E(V)$) curves for each of the constituent elements occupying the coloring site for both the (c) hexagonal and (e) cubic phases. (d) Comparison of the lowest-energy coloring patterns for the hexagonal and cubic phases, given as differences relative to the energy of the optimized cubic geometry.

Although previously unreported, the existence of polytypism in Nowotny–Juza phases is not entirely surprising. These phases are usually described as comprising a wurtzite or zinc blende substructure of groups II and V elements stuffed with a monovalent closed-shell group I cation. Because these tetrahedral nets are isostructural and isoelectronic with classic eight-electron semiconductors, one could expect a low energy barrier for rearrangement of this structural component.[7] To probe the energy difference between the hexagonal and cubic polytypes, the Vienna Ab Initio Simulation Package (VASP) was used.[8,9]

The VASP calculations used projected augmented-wave (PAW) pseudopotentials.[10] A conjugated algorithm was applied to the structural optimization with an 11 × 11 × 11 Monkhorst–Pack k-point grid.[11] During structural optimizations, atomic coordinates as well as cell volumes were allowed to relax, except for the energy versus volume ($E(V)$) curves, during which the cell volume was fixed. Total energies were calculated using the tetrahedron method with Blöchl corrections applied.[12] The VASP calculations treated exchange and correlation by either the local density approximation (LDA) or the Perdew–Burke–Ernzerhof (PBE)[13] generalized gradient functional in the case of total energy calculations. To estimate accurate gaps from the band structures, the Tran–Blaha-modified Becke–Johnson (TB-mBJ) potential was utilized.[14,15] Transport properties were calculated using the rigid-band approximation and constant scattering time approximation as implemented by the BoltzTraP code.[16] For these calculations, a much denser 41 × 41 × 41 k-point grid was used with the TB-mBJ potential because of the importance of an accurate band gap for transport property calculations. Denser k meshes were used but found to yield similar results.

The experimentally reported hexagonal crystal structure of LiZnSb comprises a (ZnSb) wurtzite-type net stuffed with lithium. The analogous cubic polytype would comprise a (ZnSb) zinc blende framework stuffed with lithium. However, unlike the hexagonal case, where the two wurtzite network positions have similar coordination environments, these two sites are inequivalent in the zinc blende substructure (Figure 2): one site, 4c, has a heterocubic coordination environment formed by two tetrahedral surroundings to the other two constituent elements; the other site, 4b, has tetrahedral coordination to the 4c site and octahedral coordination to the Li 4a site. Because of this, the choice of coloring pattern,[17,18] i.e., the distribution of elements among possible crystallographic sites, greatly impacts the total energy. To examine this question, $E(V)$ curves were plotted for the cubic and hexagonal polytypes while retaining the stoichiometry and symmetry (Figure 2).

The lowest-energy coloring pattern for hexagonal LiZnSb agrees with experimental observations from prior solid-state synthesis of the bulk material. Having either Zn or Sb occupying the 2a site in a Li-based wurtzite structure is found to be highest in energy (Figure 2c). Similarly, in the cubic case, having lithium occupy the 4c site and be involved in the polar-covalent zinc blende network is not preferred (Figure 2e). Although not as unfavorable as Li, having Sb occupy the 4c site is also energetically unfavorable. This is contrary to other cubic LiZnPn (Pn = N, P, As) Nowotny–Juza phases known in the bulk, which show a preference to have the pnictide occupy the heterocubic site.[19,20] In fact, cubic LiZnSb is the first instance of a Nowotny–Juza phase with the group II element occupying the 4c site (see below).

To ensure the validity of this coloring approach, $E(V)$ curves were generated for a larger, comprehensive family of pnictide-containing cubic Nowotny–Juza phases (see Table S2). In all cases for which an experimental bulk cubic crystal structure is known, this agrees with the lowest-energy calculated coloring pattern. The transition in cubic site preference occurs upon moving to the heavier pnictides (Sb and Bi). However, only the hexagonal phases of both LiZnSb and LiZnBi have previously been reported.

Along with a considerable energy difference, noticeable changes in lattice parameter are expected between coloring

DOI: 10.1021/jacs.6b10054
J. Am. Chem. Soc. 2016, 138, 14574–14577

patterns. The theoretical *a* lattice parameter for cubic LiZnSb, calculated using the LDA, is 6.14 Å (Figure 1), which is slightly (1.4%) smaller than the experimental lattice constant of 6.23 Å obtained from Rietveld refinement. This agrees with the extent (1.4 ± 1.2%) to which LDA underestimates the known experimental lattice parameters of other previously reported pnictide-containing cubic Nowotny–Juza phases (see Table S1). LDA also underestimates (by 2.03%) the lattice parameters of hexagonal LiZnSb. In other words, the slightly low estimate of the lattice parameter for Zn occupying the 4c site is consistent with the limitations of this method and in line with similar low estimates obtained by LDA in other classes of compounds.[21] On the basis of this comparison between the calculated cubic lattice parameter and powder XRD data, along with the energy difference between coloring patterns, we can assign Zn to the 4c site, despite the fact that prior LiZnPn structures have always preferred the pnictide to be on the 4c site. This site preference is not trivial because the lattice constant and the band structure (see Figure S1) are affected. In particular, the value and nature of the band gap as well as the lowest-energy conduction bands change with coloring. With Zn in the 4c site, cubic LiZnSb has an indirect band gap of 1.2 eV, whereas with Sb in this site, the material has a direct band gap of 1.3 eV. These differences significantly alter the transport properties (see below).

Having determined its crystal structure and most favorable site preference allows a comparison of the energy of the new cubic LiZnSb phase to that of the hexagonal polytype. As shown in Figure 2d, cubic LiZnSb is energetically preferred across all unit cell volumes. This result is surprising because it suggests that the thermodynamically less stable hexagonal phase forms at high temperature (in the bulk). However, all of the calculations were performed on stoichiometric phases, whereas on the basis of past experiments bulk hexagonal LiZnSb is known to be an unintentionally p-type doped and, likely, nonstoichiometric semiconductor.[4] These computational results provide a rationale for the extreme difficulty researchers have faced while trying to synthesize stoichiometric or n-type compositions of LiZnSb using high-temperature synthesis.

The calculated transport properties and thermoelectric efficiencies of cubic LiZnSb at 600 K with either Zn or Sb occupying the heterocubic 4c site are shown in Figure 3. In both cases, the large Seebeck coefficients give rise to impressive power factors of over 110 μW cm^{-1} K^{-2} s^{-1}. However, when Sb occupies the 4c site, the peak power factor occurs at a doping level that is too high to be useful (even at 0.3 electrons/unit cell the power factor is still below 80 μW cm^{-1} K^{-2} s^{-1}). In contrast, when Zn occupies this site, the power factor increases much more abruptly with doping. As a result, even though Sb coloring has a slightly higher power factor, the thermal conductivity becomes too large, yielding a smaller zT value. By treating the electronic thermal conductivity according to the Wiedemann–Franz law, in which the Lorentz number is determined by the Seebeck coefficient,[22] zT can be calculated without knowing the electronic component of the thermal conductivity. The benefit of this approach is that every variable, with the exception of κ_l/τ, can be obtained directly from the band structure.

The large zT found for n-type cubic LiZnSb is on a similar scale as that for the hexagonal polytype (see the Supporting Information for additional operating temperatures and the calculations repeated using PBE for direct comparison with past hexagonal LiZnSb calculations). However, as has been

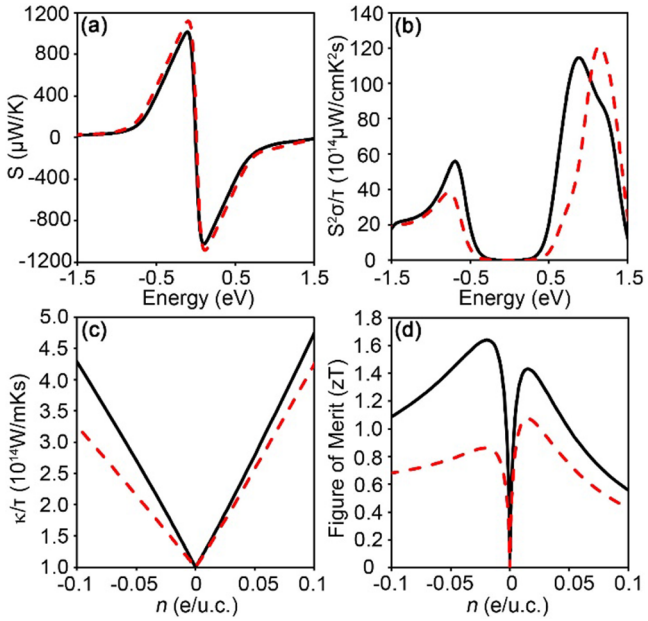

Figure 3. Thermoelectric properties of cubic LiZnSb at 600 K calculated using TB-mBJ with both Zn (black, solid) and Sb (red, dashed) occupying the 4c site. (a, b) Plots of (a) Seebeck coefficient and (b) thermopower vs the Fermi level have the Fermi level placed directly in the middle of the band gap. (c, d) Plots of (c) thermal conductivity and (d) zT vs doping are given so that negative and positive doping levels correspond to n- and p-type materials, respectively.

demonstrated for the hexagonal case and other Sb-based Zintl phases, the synthesis of these compounds generally yields the p-type analogues (likely because of vacancies, as discussed before).[4] This makes the large zT for p-type cubic LiZnSb especially promising.

To calculate zT, a common value of 1 × 10^{14} W K^{-1} m^{-1}s^{-1} was assumed for κ_l/τ, which makes a comparison with prior calculations on the hexagonal polytype more straightforward.[3] This assumption agrees well with experimental measurements on p-type hexagonal LiZnSb.[4] An added benefit of the solution-phase preparation of cubic LiZnSb is the tendency for hot-injection methods to give reduced grain size, which causes a reduction in lattice thermal conductivity. This lowering of the lattice thermal conductivity by nanostructuring makes the assumption of κ_l/τ = 1 × 10^{14} W K^{-1} m^{-1}s^{-1} relatively conservative and not overly optimistic.[1] Thus, combining solution-phase synthesis and nanostructuring to reduce the thermal conductivity could keep the extremely high power factor and place cubic LiZnSb among the most efficient thermoelectric materials for both n- and p-type compositions. Furthermore, its constituent elements and low-temperature synthesis make LiZnSb promising from both a cost and a toxicity perspective.

In summary, our results address the difficulty in synthesizing n-type or even stoichiometric compositions of the suggested hexagonal LiZnSb for thermoelectric applications. Furthermore, by the use of low-temperature solution-phase methods, the first instance of polytypism within Nowotny–Juza phases has been demonstrated. This cubic polytype shows the first example of a group II element occupying the heterocubic site, which has important implications for its band structure and, ultimately, its transport properties. The extremely high power factor of cubic LiZnSb at 600 K results in promising zT values for both n- and

DOI: 10.1021/jacs.6b10054
J. Am. Chem. Soc. 2016, 138, 14574–14577

p-type doping of over 1.6 and 1.4, respectively. This result uses a conservative estimate for the lattice thermal conductivity, an estimate that can likely be reduced by nanostructuring. We hope that this report sparks additional investigation into the development of cubic LiZnSb for thermoelectric applications.

■ ASSOCIATED CONTENT

Supporting Information

The Supporting Information is available free of charge on the ACS Publications website at DOI: 10.1021/jacs.6b10054.

Further experimental and computational details (PDF)

■ AUTHOR INFORMATION

Corresponding Authors

*vela@iastate.edu

*gmiller@iastate.edu

Notes

The authors declare no competing financial interest.

■ ACKNOWLEDGMENTS

J.V. thanks the U.S. National Science Foundation for a CAREER Grant from the Division of Chemistry, Macromolecular, Supramolecular, and Nanochemistry Program (1253058). Computations were performed on cluster funded by the College of Liberal Arts and Sciences Computational Advisory Committee (LASCAC) at Iowa State University (202-04-36-03-1000), with additional support from the Chemistry Department.

■ REFERENCES

(1) Snyder, G. J.; Toberer, E. S. *Nat. Mater.* **2008**, *7*, 105−114.

(2) Jain, A.; Shin, Y.; Persson, K. A. *Nat. Rev. Mater.* **2016**, *1*, 15004.

(3) Madsen, G. K. H. *J. Am. Chem. Soc.* **2006**, *128*, 12140−12146.

(4) Toberer, E. S.; May, A. F.; Scanlon, C. J.; Snyder, G. J. *J. Appl. Phys.* **2009**, *105*, 063701.

(5) Andaraarachchi, H. P.; Thompson, M. J.; White, M. A.; Fan, H.-J.; Vela, J. *Chem. Mater.* **2015**, *27*, 8021−8031.

(6) White, M. A.; Thompson, M. J.; Miller, G. J.; Vela, J. *Chem. Commun.* **2016**, *52*, 3497−3499.

(7) Yeh, C.-Y.; Lu, Z. W.; Froyen, S.; Zunger, A. *Phys. Rev. B: Condens. Matter Mater. Phys.* **1992**, *46*, 10086−10097.

(8) Kresse, G.; Furthmüller, J. *Comput. Mater. Sci.* **1996**, *6*, 15−50.

(9) Kresse, G.; Furthmüller, J. *Phys. Rev. B: Condens. Matter Mater. Phys.* **1996**, *54*, 11169−11186.

(10) Kresse, G.; Joubert, D. *Phys. Rev. B: Condens. Matter Mater. Phys.* **1999**, *59*, 1758−1775.

(11) Monkhorst, H. J.; Pack, J. D. *Phys. Rev. B* **1976**, *13*, 5188−5192.

(12) Blöchl, P. E. *Phys. Rev. B: Condens. Matter Mater. Phys.* **1994**, *50*, 17953−17979.

(13) Perdew, J. P.; Burke, K.; Ernzerhof, M. *Phys. Rev. Lett.* **1996**, *77*, 3865−3868.

(14) Becke, A. D.; Johnson, E. R. *J. Chem. Phys.* **2006**, *124*, 221101.

(15) Tran, F.; Blaha, P. *Phys. Rev. Lett.* **2009**, *102*, 226401.

(16) Madsen, G. K. H.; Singh, D. J. *Comput. Phys. Commun.* **2006**, *175*, 67−71.

(17) Burdett, J. K.; Lee, S.; McLarnan, T. J. *J. Am. Chem. Soc.* **1985**, *107*, 3083−3089.

(18) Miller, G. J. *Eur. J. Inorg. Chem.* **1998**, *1998*, 523−536.

(19) Bende, D.; Grin, Y.; Wagner, F. R. *Chem. - Eur. J.* **2014**, *20*, 9702−9708.

(20) Bende, D.; Wagner, F. R.; Grin, Y. *Inorg. Chem.* **2015**, *54*, 3970−3978.

(21) Haas, P.; Tran, F.; Blaha, P. *Phys. Rev. B: Condens. Matter Mater. Phys.* **2009**, *79*, 085104.

(22) Kim, H.-S.; Gibbs, Z. M.; Tang, Y.; Wang, H.; Snyder, G. J. *APL Mater.* **2015**, *3*, 041506.

DOI: 10.1021/jacs.6b10054
J. Am. Chem. Soc. 2016, 138, 14574−14577